Nigerian Journal of Physics (NJP)
ISSN online: 3027-0936
ISSN print: 1595-0611
DOI: https://doi.org/10.62292/njp.v33i1.2024.202
Volume 33(1), March 2024

Comparative Assessment of Optical and Solid-State Characteristics in Antimony-Doped Chalcogenide Thin Films of ZnSe and PbSe to Boost Photovoltaic Performance in Solar Cells

***[1]Nworie, I. C., [2]Ishiwu, S. M. U., [1]Agbo, P. E., [1]Ojobeagu, A. O., [1]Otah, P. B., [3]Mbamara, C. and [4]Ojobo, B.**

[1]Department of Industrial and Medical Physics, David Umahi Federal University of Health Sciences Uburu, Ebonyi State, Nigeria
[2]Department of Industrial Physics, Ebonyi State University, Abakaliki Nigeria
[3]Department of Industrial Physics, University of Agriculture and Environmental Science, Umuagwo, Imo State, Nigeria
[4]Department of Physics and Astronomy, University of Nigeria, Nsukka

[*]Corresponding author's email: nworieikechukwuc@gmail.com

ABSTRACT

Solar cell efficiency is crucial for maximizing the potential of solar energy as a sustainable power source. This research investigates the optical and solid-state properties of antimony-doped ZnSe and PbSe thin films using the spray pyrolysis technique. The process involves meticulous cleaning of soda-lime glass substrates, deposition of precursors (antimony chloride ($SbCl_3$), lead chloride ($PbCl_2$), hydrated zinc acetate (Zn (CH_3COO) •$3H_2O$), and sodium selenosulfide ($NaSeSO_3$) via nebulizer-driven atomization onto heated substrates at a temperature of 80°C, and subsequent annealing at 300°C in a controlled nitrogen atmosphere for 60 minutes, facilitated by a tube furnace. Optical property evaluation through UV-Vis spectrophotometry reveals intriguing trends, such as a decrease in absorbance and an ascending transmittance with elongated wavelengths. Annealed films exhibit peak optical conductivity values around the visible spectrum, and augmented refractive indices correlate with increased wavelengths, further enhanced through annealing. Antimony doping influences band gap energy, making these materials promising for solar cell fabrication. This study underscores the potential of antimony-doped ZnSe and PbSe thin films to enhance solar cell efficiency. The films offer features like enhanced light trapping, lowered band gap energy, and improved charge transport characteristics, making them suitable for various solar cell applications, including antireflection coatings and light-trapping layers. Continued exploration and refinement of these materials are anticipated to lead to novel advancements in solar cell design and manufacturing, contributing to more efficient and impactful energy conversion techniques.

Keywords:
Chalcogenide,
Lead,
Antimony,
Solar cell,
Band gap energy.

INTRODUCTION

In recent times, the global energy landscape has undergone a substantial transformation driven by an urgent need to combat climate change and reduce reliance on fossil fuels. Among the array of renewable energy sources, solar energy has emerged as a promising solution for clean and sustainable power generation. To unlock the full potential of solar energy, advancements in photovoltaic technology are essential. A pivotal avenue to enhance solar cell efficiency lies in the exploration of novel materials and innovative thin film configurations. In this realm, the intriguing prospects of antimony-doped chalcogenide thin films, specifically those composed of Zinc Selenide (ZnSe) and Lead Selenide (PbSe), have come to the forefront due to their unique optical and solid-state properties.

The escalating demand for sustainable and renewable energy sources has catalyzed extensive research within the domain of solar cell technology (Ganiyu *et al.*, 2020). In this pursuit, thin-film solar cells have emerged as a promising pathway for efficiently and economically converting sunlight into electricity. Among the diverse materials under scrutiny for thin-film solar cells, chalcogenide semiconductors have attracted substantial attention (Amrillah *et al.*, 2023). Their tunable

bandgaps, favorable optoelectronic attributes, and potential for elevating solar cell efficiency have positioned them as notable contenders. Remarkably, the strategic incorporation of antimony (Sb) dopants has been explored to further enhance the performance of these chalcogenide thin films, with ZnSe and PbSe emerging as particularly promising candidates. Chalcogenide semiconductors characterized by the fusion of chalcogen (S, Se, and Te) elements with metals, exhibit captivating traits such as direct bandgap transitions, substantial absorption coefficients, and compatibility with cost-effective fabrication techniques (Yao *et al.*, 2019). These attributes render them auspicious candidates for absorber materials in thin-film solar cells. Their capacity to adjust their bandgap to align with the solar spectrum and facilitate efficient charge carrier transport has propelled chalcogenides to the forefront of photovoltaic materials research (Chatterjee *et al.*, 2022, Amrillah *et al.*, 2023).

ZnSe and PbSe, both semiconductor materials, showcase remarkable optoelectronic characteristics, rendering them well-suited for photovoltaic applications. Their direct bandgaps empower them to efficiently capture photons across a broad solar radiation spectrum (Kulkarni et al., 2022, Ganiyu *et al.*, 2020 & Amrillah *et al.*, 2023). Nonetheless, despite their inherent potential, challenges such as limited light absorption and carrier mobility can impede their photovoltaic efficacy. To surmount these hurdles and unlock maximal solar cell efficiency, the integration of antimony (Sb) dopants into these chalcogenide materials has garnered substantial attention. Antimony, acting as a donor impurity, introduces additional energy levels within the bandgap (Charoenphon *et al.*, 2023), thereby altering the host material's electronic structure. This modulation holds the potential to enhance carrier generation, transport, and collection efficiencies. Through meticulous control of antimony doping levels, the optical and solid-state attributes of ZnSe and PbSe thin films can be precisely tailored to optimize their function as absorber layers in solar cells.

ZnSe is a preferred material for lenses (Nazar, 2014, Amrillah *et al.*, 2023, and Chatterjee *et al.*, 2022), window layers and output couplers for its low absorptive at infra-red wavelengths and its visible transmission (Amrillah *et al.*, 2023, Chatterjee *et al.*, 2022). Nano based zinc selenide thin films with a wide direct band gap (3.87) has a high transmittance in the visible region having great interest in practical applications in optoelectronics and photonic (Christian et al., 2022, Nazar, 2014). Antimony-doped thin films of ZnSe and PbSe can be deposited using a variety of methods, including thermal evaporation, self assembly technique, spray pyrolysis, electron beam evaporation, and solution growth technique.etc (Tiwari, 2012, Nazar, 2014). This research's primary objective is to conduct a comprehensive comparative analysis of the optical and solid-state characteristics of antimony-doped chalcogenide thin films, focusing on ZnSe and PbSe, to facilitate heightened solar cell efficiency. By unraveling the intricate relationships binding antimony doping, optical properties, and charge transport dynamics, this study aspires to contribute critical insights to the advancement of strategies for designing more efficient and economically viable solar cells. Ultimately, the knowledge gained from this comprehensive analysis is poised to propel innovative approaches in solar energy conversion, steering the global transition toward a sustainable and environmentally benign energy future.

In this present work, Antimony-doped thin films of ZnSe and PbSe thin films were deposited using spray pyrolysis technique and annealed. The samples were characterized using Spectrophotometer.

Theory

Absorbance (A)

Absorbance is the quantity directly determined from absorption spectra measurement and the instrument scales are often calibrated in this unit (au). By definition,

$$A = \log\left({}^{I_O}/_{I}\right) = log_{10}\left({}^{I}/_{T}\right) \quad (1a)$$

$$A = 2 - log_{10}(\%T) \quad (1b)$$

Where I_O and I are the incident and transmitted intensities respectively. According to (Rahman, 2014, Charoenphon *et al.*, 2023), absorbance and absorption coefficient (a) are related thus;

$$a = \frac{Ac}{v} \quad (2)$$

Where c and v represent the velocity of light and the frequency of the electromagnetic wave, respectively. Absorbance can be calculated from transmittance or percentage transmittance using equations 1a and 1b.

Transmittance (T)

When an electromagnetic wave, like light, crosses the interface between two different materials—such as a thin film and glass—some of the light is reflected from the inner surface, while a portion of the electromagnetic wave is refracted through the inner surface and ultimately transmitted. Reflectance represents the energy fraction reflected, whereas transmittance represents the energy fraction transmitted. Mathematically, transmittance of the specimens is defined as the ratio of the intensity (flux) of the transmitted light (I) to the intensity (flux) of the incident light (I_O).

$$T = {}^{I}/_{I_O} \quad (3)$$

The absorbance A is the logarithm of the reciprocal of the transmittance. Hence, from equation (6) we can deduce transmittance from absorbance in the form,

$$T = 10^{-A} \quad (4)$$

Thus, when one is known, the other can be determined. The absorbance or transmittance of thin films is typically directly measured using a spectrophotometer during optical characterization, while other properties are derived from calculations based on these measurements. This approach is common in obtaining various properties of thin films.

Refractive index (n)

When reflectance is normal to a surface, it can be expressed in terms of refractive index and extinction coefficient, thus,

$$R = \frac{(n-1)^2 + k^2}{(n+1)^2 + k^2} \quad (5)$$

Where n = refractive index and k = extinction coefficient. For semiconductors and insulators, k is very small i.e. $k^2 << n^2$ and equation (5) reduces to,

$$R = \frac{(n-1)^2}{(n+1)^2} \quad (6)$$

$$and \quad n = \frac{1+\sqrt{R}}{1-\sqrt{R}} \quad (7)$$

Complex index of refraction is actually used to describe the interaction of electromagnetic – radiation with matter. n has both real and imaginary part as in equation;

$$n = n - ik \quad (8)$$

Both n and k are dependent on the wavelength. The index of refraction is accurately defined as the ratio of the speed of light (c) in a vacuum to the speed (v) of the electromagnetic wave in the medium of propagation;

$$n = \frac{c}{v} \quad (9)$$

Optical conductivity (δo_p)

Optical conductivity can be defined by

$$\delta o_p = \frac{anc}{4\pi} \quad (10)$$

Where, C is the speed of light.

Optical conductivity pertains to the conductivity at the specific optical frequency under consideration, and it typically differs from the direct current (d.c) or low frequency conductivity. In metals, both δ and k values are notably high, resulting in a reflectance that approaches unity. In semiconductors, k is lower, δ is reduced, and the reflectance is also diminished, leading to higher transparency compared to metals. For insulators, k assumes a very small value, causing the dielectric constant to tend towards n^2 or $n = \sqrt{\varepsilon}$.

Band gap (E_g)

The band gap is a solid-state property and stands as a significant parameter in material characterization. Understanding optical absorption is essential in investigating the band gap. Photon-induced electronic transitions can occur either between different energy bands, leading to the determination of the energy band gap, or within a single band, such as free-carrier absorption. The band gap signifies the energy difference between the lowest point of the conduction band and the highest point of the valence band. In simpler terms, it represents the energy needed for an electron to shift from the valence band to the conduction band.

The shape of the absorption spectrum and the dispersion near the fundamental absorption edge stem from electron transitions between the upper portion of the valence band and the lower part of the conduction band (Rahman, 2014, Yao *et al.*, 2019, Nazar, 2014). These electron transitions can be categorized as direct or indirect. A transition is direct when there is no photon involvement and no change in the crystal momentum of an electron. Conversely, it is deemed indirect when the interaction with a photon leads to a significant alteration in the crystal momentum. Different types of transitions result in distinct frequency dependencies of the absorption coefficient near the absorption edge.

According to references (Amrillah *et al.*, 2023, Tiwari, 2012), the absorption coefficient for a direct transition is described as follows:

$$ahv \propto (hv - E_g)^{\gamma} \quad (11)$$

Where γ = ½ if the transition between the upper part of the valence band to the lower part of conduction band are allowed by the selection rules and γ = 3/2, the transitions are forbidden. Hence,

$$ahv = A(hv - E_g)^{1/2} \quad (12$$

For allowed transitions, that is

$$(ahv)^2 = B(hv - E_g) \quad (13)$$

In most cases, indirect transitions (Chatterje *et al.*, 2022) are weaker than direct ones by 2 or 3 orders of magnitude. This is because they arise from second-order perturbation only and are observable only in energy regions devoid of direct transitions. The relationship between the absorption coefficient and the energy of light quanta near the fundamental edge is described by equations 12 and 13.

A plot of α^2 against hv yields a linear graph with the negative band gap serving as the intercept. However, within the absorption edge region, the absorption diminishes to such low values that measuring the portion attributed to band-to-band transitions becomes challenging. This difficulty arises from the potential masking of the transition by other incidental absorption or losses in the specimens or experimental equipment. Consequently, a plot of α^2 versus hv does not usually exhibit a straight pattern in the absorption edge region. Therefore, the intercept providing the band gap is extrapolated from the linear section of the graph to the relevant point.

$$a^2 = 0 \quad (14)$$

[10] Discovered that in some compounds, the density of impurities affected the position of the absorption edge in such a way as to shift it to a shorter wavelength and this causes a large increase in the band gap of such material.

In joules, the photo energy for a given wavelength in meters is given by,

$$E = hv = {}^{hc}/_{\lambda} \quad (15)$$

Where, h = plank's constant, c = velocity of light, λ = wavelength in meter (m), and v = frequency of the radiation .

If λ is in nm,

$$hv\ (ev) = \frac{1241}{\lambda} \quad (16)$$

Equation (16) is used in this study in calculating the photon energies in eV for various wavelengths, λ in nm.

MATERIALS AND METHODS

Soda-lime glass substrates served as the initial substrate material. These substrates underwent a sequential cleaning process involving acetone, isopropanol, and deionized water within an ultrasonic bath. Subsequently, the substrates were dried using a stream of nitrogen gas. Antimony chloride ($SbCl_3$) was used as the source of antimony. Additionally, lead chloride ($PbCl_2$) was employed as the lead source, and hydrated zinc acetate ($Zn(CH_3COO) \cdot 3H_2O$) was chosen as the precursor for zinc. The selenium source utilized was sodium selenosulfide ($NaSeSO_3$). Distilled water served as the reaction medium.

The deposition process took place within a custom-built Spray Pyrolysis chamber. Separate 100 ml beakers contained 20 ml of 0.7M $SbCl_3$, $PbCl_2$, $NaSeSO_3$, and $Zn(CH_3COO) \cdot 3H_2O$ dissolved in a solvent mixture of methanol and distilled water, yielding precursor solutions. The precursor solution underwent atomization into fine droplets through a nebulizer and was then sprayed onto the heated substrate. The substrate temperature was meticulously maintained at 80°C throughout the deposition process. A nitrogen carrier gas was introduced to facilitate the transportation of precursor droplets.

Furthermore, a subset of the deposited films underwent annealing at 300 degrees Celsius under a controlled nitrogen atmosphere for 60 minutes. The annealing procedure was conducted within a tube furnace to induce crystallization and optimize film properties. The balanced chemical equation of formation of Antimony-Doped Zinc Selenide (Sb-doped ZnSe) is

$$SbCl_3 + Zn(CH_3COO)_2 + Na_2SeSo_3 \longrightarrow \text{Zn}\ (1-\text{x})Sb(x)\text{Se} + \text{NaCl} + CH_3\,\text{COOH} + SO_2$$

While the balanced chemical equation of formation of Antimony-Doped lead Selenide (Sb-doped PbSe) is

$$SbCl_3 + PbCl_2 + Na_2SeSo_3 \longrightarrow \text{Pb}\ (1-\text{x})Sb(x)\text{Se} + 2\text{NaCl} + SO_2$$

where x, represents the fraction of antimony (Sb) doping in ZnSe and in PbSe respectively.

To assess the optical characteristics, UV-Vis spectrophotometry was employed to analyze the films' transmittance and absorbance properties from which other parameters were determined.

RESULTS AND DISCUSSION

Optical Characterization

UV-Vis Spectroscopy

Absorbance and transmission spectra were acquired for the antimony-doped thin films of ZnSe and PbSe samples across the ultraviolet (UV), visible, and infrared (IR) regions spanning from 200 to 1100 nm. This was accomplished using a UV-VIS-NIR PerkinElmer spectrophotometer, model Lambda 950, equipped with UV WinLab software. The instrument directly measures the sample's transmission. Utilizing the %T (percent transmission) data, all additional optical parameters were subsequently computed.

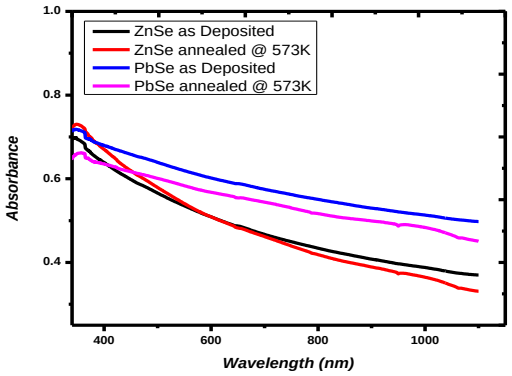

Figure 1: Absorbance Vs wavelength for ZnSe and PbSe thin films as deposited and annealed @573K

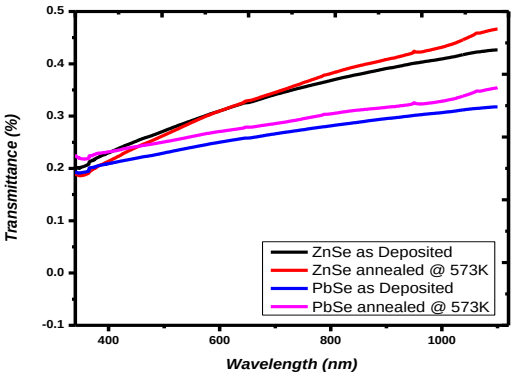

Figure 2: Transmittance Vs wavelength for ZnSe and PbSe thin films as deposited and annealed @573K

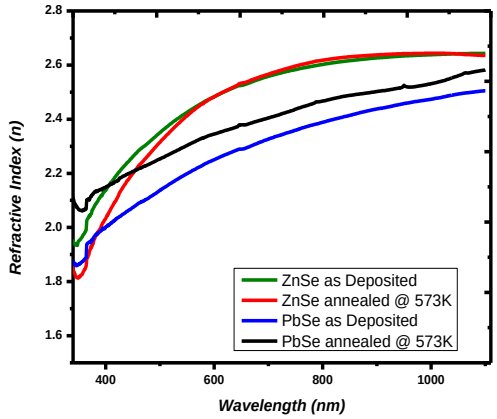

Figure 3: Refractive IndexVs wavelength for ZnSe and PbSe thin films as deposited and annealed @573K

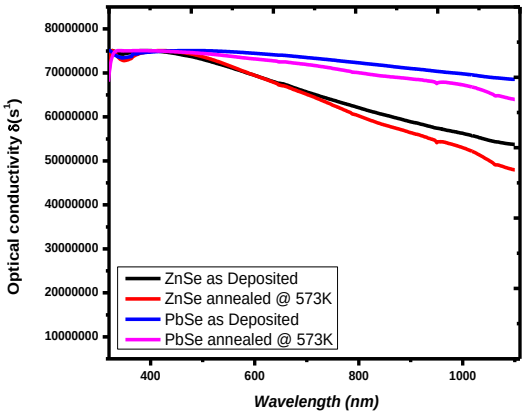

Figure 4: Optical Conductivity Vs wavelength for ZnSe and PbSe thin films as deposited and annealed @573K

The graph presented in Figure 1 illustrates that both deposited ZnSe and PbSe thin films exhibit a reduction in absorbance as the wavelength increases. The peak absorbance value is observed at 0.74 for the ZnSe film annealed at 573K, while the lowest value of 0.66 is recorded for the PbSe film annealed at 573K. The transmittance values for both deposited and annealed ZnSe and PbSe thin films exhibit an increasing trend with longer wavelengths, ranging from 300nm to 1100nm, as illustrated in Figure 2. Within the visible and infrared regions, the transmittance varies between 15% and 90%. Among the samples, the highest transmittance values were observed for annealed ZnSe film at 573K and the lowest for as-deposited PbSe. The increasing trend of transmittance with longer wavelengths in ZnSe and PbSe thin films suggests that they could play a beneficial role in improving solar cell efficiency by enhancing light absorption, reducing reflectance losses, enabling broadband light harvesting, aiding thermal management, and facilitating advanced tandem cell architectures. A material with increasing transmittance with longer wavelengths could find application as an antireflection coating in solar cells (Baryshnikova *et al.*, 2016), particularly in the visible and infrared regions, where efficient light absorption is crucial for energy conversion.

As depicted in Figure 3, a clear trend emerges wherein the index of refraction values for the deposited ZnSe and PbSe thin films rise with increasing wavelengths. Additionally, the process of annealing the films results in an augmentation of the refractive index for both ZnSe and PbSe materials. The range of refractive indices for all the deposited films spans from 1.82 to 2.85. Notably, the highest refractive index is observed at 2.85 for annealed ZnSe films, while for annealed PbSe films, it reaches a peak of 2.75. These findings underline the influence of wavelength and annealing on the optical properties of the thin films. The observed increase in refractive indices due to annealing, coupled with the range of values obtained, suggests that these thin films have the potential to enhance solar cell efficiency through improved light trapping, antireflection coatings, increased photon path length, and innovative tandem cell configurations. It can be used as Transparent Conductive Layers, Antireflection Coatings (ARCs), Light-Trapping Layers (VeluKaliyannam *et al.*, 2019, Baryshnikova *et al.*, 2016). It could also find use in other optoelectronic devices, such as photodetectors or light-emitting devices, where controlling the interaction of light with materials is essential.

The plot of figure 4 revealed a distinct trend: optical conductivity consistently diminishes within the infrared region of the spectrum as wavelengths increase across all deposited films. Notably, the films exhibited their peak optical conductivity values around the visible spectrum upon undergoing annealing. Particularly, PbSe films annealed at 573K demonstrated higher optical conductivity compared to ZnSe films under the same annealing conditions. This elevated value could potentially be attributed to specific factors at play such as the crystalline quality achieved through annealing (Liu *et al.*, 2014), the formation of defect states, modifications in the band structure, or variations in carrier concentration. This has called for further investigation to precisely elucidate the underlying mechanisms responsible for this observed enhancement in optical conductivity.

The band gap energies of the ZnSe and PbSe thin films depicted in Figure 5 span a range from 1.57 eV to 1.87 eV. Specifically, the band gap energies are as follows: 1.57 eV for PbSe annealed at 573K, 1.71 eV for un-annealed PbSe, 1.82 eV for ZnSe annealed at 573K, and 1.87 eV for as-deposited ZnSe.

It is noteworthy that the introduction of antimony doping has led to a reduction in the band gap energy of these materials. This alteration in the band gap makes the materials well-suited for solar cell fabrication (Christian *et al.*, 2022, Tiwari, 2012), as reduction in

energy necessary to transfer an electron from upper valence level to the conduction level increases the overall efficiency of light-to-energy conversion in solar cell.

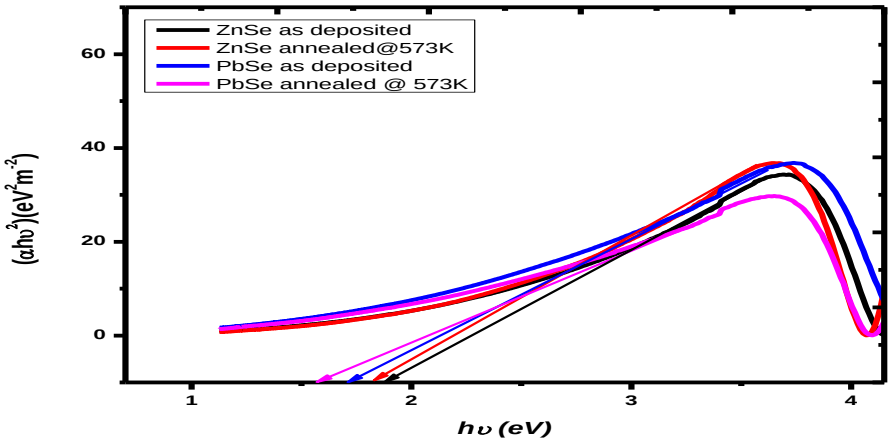

Figure 5: plot of $(\alpha h\nu)^2$ verses *hv* for ZnSe and PbSe thin films as deposited and annealed @573K

CONCLUSION

In conclusion, our comparative study of antimony-doped ZnSe and PbSe thin films, utilizing the spray pyrolysis technique, has illuminated their potential for enhancing solar cell efficiency. These materials exhibit favorable optical and solid-state properties, including improved light trapping, reduced band gap energy, and enhanced charge transport characteristics. These findings indicate that the films could play a vital role in various aspects of solar cell technology, such as antireflection coatings, light-trapping layers, and more efficient charge carrier dynamics. Further exploration and optimization of these materials could lead to innovative advancements in solar cell design and manufacturing.

DATA AVAILABILITY STATEMENT

The data that support the findings of this study are available from the corresponding author upon reasonable request.

REFERENCES

Amrillah, T., Prasetio, A., Supandi, A. R., Sidiq, D. H., Putra, F. S., Nugroho, M. A., & Azmi, R. (2023). Environment-friendly copper-based chalcogenide thin film solar cells: status and perspectives. *Materials Horizons*, *10*(2), 313-339. https://doi.org/10.1039/D2MH00983H

Baryshnikova, K. V., Petrov, M. I., Babicheva, V. E., & Belov, P. A. (2016). Plasmonic and silicon spherical nanoparticle antireflective coatings. Scientific reports, 6(1), 22136 https://www.nature.com/articles/srep22136 doi: 10.1038/srep22136 (2016).

Charoenphon, S., Tubtimtae, A., Watanabe, I., Jungthawan, S., Jiraroj, T., Boonchun, A., & Reunchan, P. (2023). The role of native point defects and donor impurities in the electrical properties of ZnSb 2 O 4: a hybrid density-functional study. *Physical Chemistry Chemical Physics*, *25*(28), 19116-19125. https://doi.org/10.1039/D3CP01470C

Chatterjee, P., Ambati, M. S. K., Chakraborty, A. K., Chakrabortty, S., Biring, S., Ramakrishna, S., & Dalapati, G. K. (2022). Photovoltaic/photo-electrocatalysis integration for green hydrogen: A review. *Energy Conversion and Management*, *261*, 115648. https://doi.org/10.1016/j.enconman.2022.115648

Christian, N. I., Ekuma, A. P., Kingsley, O., & Ugah, J. O. (2023). ENERGY AND ECONOMIC EVALUATION OF THE 3000KWP GRID CONNECTED PHOTOVOLTAIC POWER PLANT IN UMUOGHARA QUARRY INDUSTRIAL CLUSTER, NIGERIA. *The Journals of the Nigerian Association of Mathematical Physics*, *65*, *21-26*. *https://nampjournals.org.ng/index.php/home/article/view/4*

Ganiyu, S. O., Martinez-Huitle, C. A., & Rodrigo, M. A. (2020). Renewable energies driven electrochemical wastewater/soil decontamination technologies: A critical review of fundamental concepts and applications. *Applied Catalysis B: Environmental*, *270*, 118857. https://doi.org/10.1016/j.apcatb.2020.118857

Kulkarni, M. B., Upadhyaya, K., Ayachit, N. H., & Iyer, N. (2022). 13 Quantum Dot–Polymer Composites in Light-Emitting Diode Applications. *Quantum Dots and*

Polymer Nanocomposites: Synthesis, Chemistry, and Applications, 259. https://www.taylorfrancis.com/chapters/edit/10.1201/9781003266518-13/

Liu, D., Lv, Y., Zhang, M., Liu, Y., Zhu, Y., Zong, R., & Zhu, Y. (2014). Defect-related photoluminescence and photocatalytic properties of porous ZnO nanosheets. *Journal of Materials Chemistry A*, *2*(37), 15377-15388. https://doi.org/10.1039/C4TA02678K

Nazar, A.S. (2014). Physical Properties of Silver Doped ZnSe Thin Films for Photovoltaic Applications. *Iranian Journal of Energy and Environment* 5 (1): 87-93, 2014 DOI: 10.5829/idosi.ijee.2014.05.01.13

Rahman, M. A. (2014). A review on semiconductors including applications and temperature effects in semiconductors. *American Scientific Research Journal for Engineering, Technology, and Sciences (ASRJETS)*, *7*(1), 50-70. http://asrjetsjournal.org/

Silva, A. B., Lima Filho, N. M., Palha, M. A., & Sarmento, S. M. (2013). Kinetics of water disinfection using UV-C radiation. *Fuel*, *110*, 114-123. https://doi.org/10.1016/j.fuel.2012.11.026

Tiwari, G. N. (2012). Solar Energy Fundamentals, Design, Modeling and Applications. New Delhi, India: Nasora Publishing House Pvt. Ltd., vii, 1,435. https://cir.nii.ac.jp/crid/1130282273051048064

Velu Kaliyannan, G., Palanisamy, S. V., Palanisamy, M., Chinnasamy, M., Somasundaram, S., Nagarajan, N., & Rathanasamy, R. (2019). Utilization of 2D gahnite nanosheets as highly conductive, transparent and light trapping front contact for silicon solar cells. Applied Nanoscience, 9, 1427-1437 DOI https://doi.org/10.1007/s13204-018-00949-4

Yao, J. D., Zheng, Z. Q., & Yang, G. W. (2019). Production of large-area 2D materials for high-performance photodetectors by pulsed-laser deposition. *Progress in Materials Science*, *106*, 100573. https://doi.org/10.1016/j.pmatsci.2019.100573